The silent earthquake of 2002 in the Guerrero seismic gap, Mexico (Mw=7.6): inversion of slip on the plate interface and some implications

(Submitted to Earth and Planetary Science Letters)

A. Iglesias[a], S.K. Singh[a], A. R. Lowry[b], M. Santoyo[a], V. Kostoglodov[a], K. M. Larson[c], S.I. Franco-Sánchez[a] and T. Mikumo[a]

[a] *Instituto de Geofísica, Universidad Nacional Autónoma de México, México, D.F., México*

[b] *Department of Physics, University of Colorado, Boulder, Colorado, USA*

[c] *Department of Aerospace Engineering Science, University of Colorado, Boulder, Colorado, USA*

Abstract. We invert GPS position data to map the slip on the plate interface during an aseismic, slow-slip event, which occurred in 2002 in the Guerrero seismic gap of the Mexican subduction zone, lasted for ~4 months, and was detected by 7 continuous GPS receivers located over an area of ~550x250 km^2. Our best model, under physically reasonable constraints, shows that the slow slip occurred on the transition zone at a distance range of 100 to 170 km from the trench. The average slip was about 22.5 cm (M_0~2.97 x10^{27} dyne-cm, Mw=7.6). This model implies an increased shear stress at the bottom of the locked, seismogenic part of the interface which lies updip from the transition zone, and, hence, an enhanced seismic hazard. The results from other similar subduction zones also favor this model. However, we cannot rule out an alternative model that requires slow slip to invade the seismogenic zone as well. A definitive answer to this critical issue would require more GPS stations and long-term monitoring.

Introduction

Recent continuous geodetic observations, made possible by widespread deployment of GPS receivers, have revealed that slow slip events or silent earthquakes on plate interfaces are a relatively common phenomenon [e.g**. 1-4**]. Such observations promise to revolutionize our understanding of the earthquake source process, interface coupling, the earthquake cycle, and the rheology of the plate interface.

Two silent earthquakes have been reported in the Guerrero seismic gap [**5 and 6**]. This gap is located along the Mexican subduction zone. It extends from 99.2^{o}W to 101.2^{o}W (Figure 1). No large subduction thrust earthquakes have occurred in the NW part of the gap since 1911 [**7**]. The region SE of Acapulco, up to 99.2^{o}W, has experienced only relatively small (Mw≤7.1) earthquakes since 1957. The entire gap is about 200 km in length. If the gap were to rupture in a single earthquake, it would give rise to an event of magnitude Mw of 8.1-8.4 [**8**]. Because such an event poses great seismic hazard to Acapulco, the state of Guerrero, and to Mexico City, this region has been instrumented with seismographs, accelerographs, and GPS receivers. Figure 1 shows the 7 permanent, continuous GPS receivers that were in operation in the region in January 2003.

The first silent earthquake occurred in 1998. It was detected by the continuous GPS receiver at *CAYA* (Figure 1), the only station in operation at the time [**5**]. The most active phase of the second, much larger, slow earthquake began in January 2002, and lasted for about four months [**6**]. It was recorded by seven continuous GPS receivers located over an area of ~550x250 km^2 (Figure 1). The data and a preliminary interpretation based on two-dimensional forward modeling were presented in a previous work [**6**]. In that work the authors conclude that the data could be interpreted by one of two extreme models. One model implies increased seismic hazard in the Guerrero gap (slip occurring only over the transition zone), while the second model points to diminished hazard (slip extending over the seismogenic zone). In this study, we formally invert the data, given physical constraints, to map the slip on the plate interface. Our goal is to resolve which of the two scenarios, increased or diminished hazard, is better supported by the data. Clearly, the issue is of critical importance because of its tectonic and seismic hazard implications.

Tectonic Setting and the Geometry of the Benioff Zone

Figure 1 shows the tectonic setting of the Guerrero seismic gap. The oceanic *COCOS* plate subducts below continental Mexico, a part of the North American (*NOAM*) plate. The rate of *COCOS* motion relative to *NOAM* is ~5.6 ± 0.21 cm/yr in the direction N35°E [**9**].

Several studies deal with the geometry of the Benioff zone below Guerrero [**10, 11, 12**]. The results of these studies share a common feature: the oceanic *COCOS* plate enters below Mexico with a small dip (~15°), begins unbending at a distance of 100 km from the trench, and becomes subhorizontal at a distance of about 150 km. Figure 1 (bottom) shows an idealized cross section based on the locations of small and moderate earthquakes and their focal mechanisms [**13**]. In this idealization, the subducted COCOS plate enters below Mexico with a dip of 17° up to a distance of 100 km from the trench and then becomes almost horizontal (dip 2°). We will use this geometry in the inversion of the GPS data.

Data

Kostoglodov et al. [**6**] presented the time series of positions, relative to McDonald Observatory (MDO), Texas; of each of the seven GPS sites. These data exhibit all sites moving NE before January 2002. At that time, the sense of motion reversed and continued to do so for ~4 months. Beginning in May 2002, the motion resumed its pre-January 2002 direction at all sites. As an example, Figure 2 shows the time series of position for the station *CAYA* during the interval January 1997 – July 2002. Silent events, one at the beginning of 1998 [**5**] and another at the beginning of 2002 [**6**], are highlighted in the figure.

To determine the change in the position of the sites, we took the coordinate time series relative to MDO, subtracted the difference in NUVEL1a velocities of the North American plate at MDO and each site, and inverted, via weighted least squares, for a best-fit line superimposed by a hyperbolic tangent function. Table 1 and Figure 1 summarize the resulting estimates of steady-state velocity and anomalous displacement. The motion during the slow-slip was not perfectly opposite to that during the steady-state phase, instead it had a significantly less strike-parallel component of motion.

Inversion for Slip

To invert for slip on the plate interface, we use the fault geometry shown in Figure 1. The strike of the fault is chosen to coincide with the middle America trench (azimuth $\phi=289^{\circ}$). The length of the fault along strike is 600 km. The horizontal projection of the fault has a width of 350 km (Figure 1). The fault is subdivided into (3x4) elements, three along strike and four in the down-dip direction. A larger number of elements is not warranted in view of the small number of observations. We denote the elements by (*i,j*), *i*=1 to 3 and *j*=1 to 4. The elements (*2,j*) coincide with the Guerrero seismic gap. We note that the widths of the elements along the down-dip direction have been chosen to reflect our current knowledge of the seismic behavior of the plate interface along the Mexican subduction zone. Quite generally, large, shallow thrust earthquakes in Mexico do not occur between the trench and a distance of ~50 km towards the coast. The seismogenic zone roughly extends from 50 km to 100 km, and the transition zone extends beyond 100 km. The element widths have been chosen to reflect this (Figure 1): 0-50 km; 50-100 km; 100-170 km; 170-350 km. Note that the division of the transition zone in two segments, 100 km to 170 km and 170 km to 350 km, is arbitrary. As Figure 1 shows there are more GPS sites in the Guerrero gap than in the adjacent regions. For this reason, we expect the slip on elements (*2,j*) to be better resolved than those on other elements.

In the inversion, the displacement from each rectangular element is calculated using closed form expressions developed by Okada [**14**]. The rake of the slip vector, λ, is taken as an unknown parameter but is assumed to be the same for each element. The displacement from slip over the elements of the fault plane may be written as:

$$u_k = \sum_{i=1}^{3}\sum_{j=1}^{4}\left(Gd_{i,j}^{k} * S_{i,j} * \boldsymbol{sin}(\lambda) + Gs_{i,j}^{k} * S_{i,j} * \boldsymbol{cos}(\lambda)\right)$$

where u_k is the displacement vector at station k, $Gd_{i,j}^{k}$ and $Gs_{i,j}^{k}$ are the displacements at station k due to the unit pure dip slip and unit pure strike slip on the (i,j) element, respectively, and $S_{i,j}$ is the slip on the (i,j) element.

We invert for slip distribution using a simulated annealing algorithm. This algorithm allows us flexibility in imposing constraints on the misfit function and to assign weights to the data. Recently, the simulated annealing algorithm has been applied to solve some inverse problems in seismology [e.g., **15,16** and **17**]. The method explores the whole model solution space using a procedure based on the equations that govern the thermodynamic process known as annealing [**18**]. Several works show that this process guides, efficiently, the search to reach a global minimum of misfit. Some details of this inversion technique may be found in Goffe et al. [**19**] and Iglesias et al. [**17**].

As misfit function to minimize, we choose an L2 norm:

$$\text{misfit} = \sqrt{\sum_{L=1}^{n}\left(u_L^{obs} - u_L^{pre}\right)^2 * w_L}$$

where, n is the number of data [n=number of components multiplied by number of stations)], u_L^{obs}, u_L^{pre} are the observed and predicted displacements for the L-th component-station and w_L (weight for each component-station) is the reciprocal of σ .

Slow-slip Phase

The data set consists of 21 values. The unknown parameters are 13, corresponding to 12 slip amplitudes on (3x4) elements and 1 slip direction. First we inverted for the slip distribution without any further constraint. The results showed a large slip on the element *(2,3)* that lies between 100 and 170 km from the trench. The slip on this element was at least twice greater than on any other element. We then performed several tests by changing the number of elements in the down-dip direction. Basically, the solutions showed that the slip on the central strip *(2,j)* (corresponding to the Guerrero seismic gap) is well resolved. The slip on the elements *(1,j)* and *(3,j)*, however, significantly changed with any change in the number of the elements, indicating that the slip distribution on these elements is not well resolved from the available data. These initial tests suggest that the solutions are unstable because of a large number of parameters (13), relatively small number of data (21), and their spatial distribution.

Before performing additional inversions, we imposed further constraints that are physically reasonable. We required that the slip on the elements *(i,1)* be equal. The same constraint was imposed on the elements *(i,4)*. These bands represent the shallowest and deepest portion of our model (Figure 1). In the initial tests, the lateral elements *(1,2), (1,3), (3,2), (3,3)* had shown significant instability due to lack of stations. For this reason, we constructed bigger blocks by setting the slip on *(1,2)* to be equal to that on *(1,3)* and the slip on *(3,2)* to be equal to that on *(3,3)*. These constraints reduced the number of free parameters from 13 to 7. Physically, the slip at the boundaries of the elements must be continuous. In our inversion, however, we have not imposed this condition. The result of the inversion is shown in Figure 3 (top). We point out that the misfit resulting from this model (10.8 cm) is similar to that from the model where slip on each of the 13 elements is free (7.9 cm). The total seismic moment release, assuming a rigidity $\mu=3.5\times10^{11}$ dyne/cm^2, is 2.97 $\times10^{27}$ dyne-cm (Mw7.6).

Figure 3 (top) shows that the slow slip was mostly confined to the element *(2,3)*. This element extends from 100 to 170 km from the trench and corresponds to the transition zone. This segment of the plate interface slipped about 22.5 cm in 4 months. The slip direction (rake) was 91°. The parameters of the slow slip on the interface can be described by the usual convention for focal mechanisms: $\varphi=288°$, $\delta=2°$, $\lambda=91°$. No slip occurred on the elements *(2,1)* and *(2,2)*. The observed position change at sites *IGUA* and *YAIG*, however, requires a slip on the element *(2,4)*. It is important to note that the amount of slip on elements *(2,3)* and *(2,4)* depends on the widths of the elements. A smaller width would result in a larger slip and vice versa.

As mentioned above, a critical question is whether the slow slip also extended over the seismogenic zone of the Guerrero gap [element *(2,2)*]. To test this possibility, we merged elements *(2,3)* and *(2,4)* together. The result of this inversion is shown in Figure 3 (middle). The slip on the two merged elements is ~11.8 cm. The slip direction is 91°. The total seismic moment release (3.05 $\times10^{27}$ dyne-cm) is very similar to the previous case. The misfit (10.8 cm) is slightly greater and the fit to the vertical components is now worse than in the previous case. Thus, the results of the inversions favor a slow slip that was mostly confined to the transition zone, in the distance range of 100 to 170 km from the trench (Figure 3, top). This is our best model.

Steady-State Phase

The data on yearly position change of GPS sites during the steady-state phase of the deformation (Table 1) were inverted using the same fault geometry and constraints as in the previous case. The slip distribution, shown in Figure 3 (bottom), suggests that in the Guerrero gap [elements *(2,j)*] the data can be explained by an average back slip [**20**] of ~4.1 cm on the plate interface between 50 and 170 km from the trench [elements *(2,2)* and *(2,3)*]. The plate interface further down dip, in the distance range of 170 to 350 km from the trench [element *(2,4)*], requires a back slip of ~1.6 cm. The back slip in this element appears to be real in view of the position change of inland sites of *IGUA* and *YAIG* (Figure 1). The inversion also shows that the elements nearest to the trench *(i,1)* requires a back slip of ~1.9 cm. The back slip on the lateral elements *(1,2)* and *(1,3)*, and *(3,2)* and *(3,3)* are ~ 6 cm and 5 cm, respectively. The direction of back slip (rake) is –108°, which is consistent with the direction of convergence of *COCOS* with respect to *NOAM* of 35°.

Discussion and Conclusions

The displacement vectors at GPS sites above the subduction zone of Guerrero, Mexico, during the steady-state phase of strain accumulation are in agreement with the relative convergence of *COCOS* with respect to *NOAM* (5.6 cm/yr towards N35°E). The inversion of the GPS data, with physically reasonable constraints, shows an almost completely locked plate interface in the distance range of 50 to 170 km from the trench and a partially locked (~35%) interface further down dip between 170 and 350 km from the trench (Figure 3, bottom). The direction of the back slip vector, -108°, is consistent with the direction of the relative convergence vector.

The reversed motion of the GPS sites, which began in January 2002 and lasted for around four months, demonstrates the occurrence of a large silent earthquake. Our best model shows that the slow slip occurred below the Guerrero seismic gap on the plate interface that extends from ~100 to 170 km (slip ~22.5 cm) and from 170 to 350 km (slip ~3.5 cm). The direction of slow slip was 91°. In this model, the slow slip did not extend over the upper, locked portion of plate interface (~50 to 100 km from the trench). Thus the slip of 22.5 cm in four months cancelled the strain accumulated on the element *(2,3)* (~100 to 170 km from the trench; Figure 3, top) during about five years of steady-state loading. This is our preferred model. A consequence of this model is an increased shear stress at the bottom of the locked interface, thus enhancing the probability of rupture of the Guerrero seismic gap in the near future. Support for this model comes from slow slip on the transition zone reported in other regions where the age and relative speed of the subducting plate is similar, e.g., Cascadia [**2**] and before 1944 Tonankai and 1946 Nankaido great earthquakes in Japan [**21**].

The alternative model, in which slow slip extends over the seismogenic zone, results in larger misfit than in the previous case. Nevertheless, we cannot discard this model on this basis alone since the difference in the misfit between the two models is significant at only about 85% confidence. If, indeed, this is the correct model, then the slow event liberated some fraction of the accumulated strain, thus diminishing the seismic hazard in the near future. This fraction cannot be estimated from the GPS data since they cover only a short time span.

Which of the two models is in better agreement with seismic history of the region? The cumulative seismic moment release in Guerrero gap as a function of time, for the period 1800-2003 is shown in Figure 4. The figure includes two sets of parallel lines both of which envelop the moment release. The slopes of these two sets of lines, 0.20×10^{27} and 0.14×10^{27}dyne-cm/yr, correspond to perfect seismic coupling (α=1.0) and partial seismic coupling (α=0.7), respectively. In computing these slopes, we have assumed a seismogenic zone with width=50 km, length=200 km, relative plate velocity=5.8 cm/yr, and rigidity $\mu = 3.5 \times 10^{11}$ dyne/cm^2. As can be seen from Figure 4, the time series is not long enough to discriminate between a fully-coupled and a partially-coupled seismogenic interface.

It will require more extensive data to map the process of strain accumulation and release in the region. If the process is non-periodic in Guerrero, as appears to be the case [**23**], then a more definitive answer may require very long-term monitoring as well.

Acknowledgments

Fruitful conversations with Javier Pacheco and Shoichi Yoshioka are acknowledged. The manuscript was reviewed by ??,???. This research was partially funded by CONACYT grants G25842-T, 37293-T, PAPIIT grant IN104801, and NSF grants EAR 9725712 and 0125618.

References

1. Heki, K., S. Miyazaki and H. Tsuji, Silent fault slip following an interplate thrust earthquake at the Japan Trench, Nature, 386, 595-597, 1997.

2. Dragert, H., K. Wang, K., and T.S. James, A silent slip event on the deeper Cascadia subduction interface. Science, 292, 1525-1528, 2001.

3. Ozawa, S., M. Murakami, and T. Tada, Time-dependent inversion study of the slow thrust event in the Nankai trough subduction zone, southwestern Japan, J. Geophys. Res., 106, 787-802, 2001.

4. Miller, M. M., T. Melbourne, D. J. Johnson and W. Q. Sumner, Periodic slow earthquakes from the Cascadia subduction zone. Science, 295, 2423, 2002.

5. Lowry, A.R., K.M. Larson, V. Kostoglodov, and R. Bilham, Transient fault slip in Guerrero, southern Mexico. Geophys. Res. Lett., 28, 3753-3756, 2001.

6. Kostoglodov, V., S.K. Singh, J.A. Santiago, S.I. Franco, K.M. Larson, A.R. Lowry, and R. Bilham, A silent earthquake in the Guerrero seismic gap, Mexico, Geophys. Res. Lett., 30, in press.

7. Singh S.K., J. Havskov and L. Astiz, Seismic gaps and recurrence periods of large earthquakes along the Mexican subduction zone, Bull. Seism. Soc. Am., 71, 827-843, 1981

8. Singh, S.K. and F. Mortera, Source-time functions of large Mexican subduction earthquakes, morphology of the Benioff zone and the extent of the Guerrero gap, J. Geophys. Res., 96, 21487-21502, 1991.

9. DeMets, C., R. Gordon, D. Argus, and R. Stein, Effect of recent revisions to the geomagnetic reversal time scale on estimates of current plate motions. Geophys. Res. Lett., 21, 2191-2194, 1994.

10. Suárez, G., T. Monfret, G. Wittlinger, and C. David, Geometry of subduction and depth of the seismogenic zone in the Guerrero gap, Mexico. Nature, 345, 336-338, 1990

11. Singh, S.K. and M. Pardo, Geometry of the Benioff zone and state of stress in the overriding plate in central Mexico, Geophys. Res. Lett., 20, 1483-1486, 1993.

12. Kostoglodov, V., Bandy, W., Domínguez, J., and Mena, M., Gravity and seismicity over the Guerrero seismic gap, Mexico. Geophys. Res. Lett. 23, 3385-3388 , 1996.

13. Pacheco, J.F. Personal Communication, 2003.

14. Okada, Y., Internal deformation due to shear and tensile faults in a half-space, Bull. Seism. Soc. Am., 82, 1018-1040, 1992.

15. Hartzell, S. and P. Liu. Determination of earthquake source parameters using a hybrid global search algorithm. Bull. Seism. Soc. Am., 85, 516-524, 1995.

16. Courboulex F., J. Virieux, A. Deschamps, D. Gibert, and A. Zollo, Source investigation of small events using empirical Green functions and simulated annealing. Geophys. J. Int., 125, 768-780, 1996.

17. Iglesias, A., V.M. Cruz-Atienza, N.M. Shapiro, and J.F. Pacheco, Crustal structure of south-central Mexico estimated from the inversion of surface-wave dispersion curves using genetic and simulated annealing algorithms, Geof. Int., 40, 181-190, 2001.

18. Kirkpatrick, S., C.D. Gellat Jr. and M.P. Vecchi, Optimization by simulated annealing. Science, 220, 671-680.

19. Goffe, W., G.D. Ferrier, and J. Rogers, Global optimization of statistical functions with simulated annealing. Journal of Econometrics, 60, 65-100, 1994.

20. Savage, J.C., A dislocation model of strain accumulation and release at a subduction zone, J. Geophys. Res., 88, 4984-4996, 1983.

21. Linde, A. T. and I. S. Sacks, Slow earthquakes and great earthquakes along the Nankai trough, Earth Planet. Sc. Lett., 203, 265-275, 2002.

22. Anderson, J. G., S. K. Singh, J. M. Espindola and J. Yamamoto, Seismic strain release in the Mexican subduction thrust, Phys. Earth Planet. Int., 58, 307-322, 1989.

23. Kostoglodov, V., S. K. Singh, W. Hutton, O. Sanchez, K.M. Larson, A.R. Lowry, How frequent are subduction aseismic slip events in Guerrero, Mexico, Seism. Res. Lett., 73, 245, 2002.

Table 1. Position change of GPS sites in southern Mexico relative to McDonald Observatory, Texas. Z is positive upward. σ is the standard deviation.

Site	**Steady-state phase (yearly)**			**Slow-event phase Jan-Apr 2002 (4 months)**		
	$\Delta N \pm \sigma_N$ (cm)	**$\Delta E \pm \sigma_E$ (cm)**	**$\Delta Z \pm \sigma_z$ (cm)**	**$\Delta N \pm \sigma_N$ (cm)**	**$\Delta E \pm \sigma_E$ (cm)**	**$\Delta Z \pm \sigma_z$ (cm)**
CAYA	1.64±0.01	1.60±0.02	1.04±0.06	-5.57±0.06	-1.76±0.09	-6.12±0.27
ACAP	1.96±0.02	1.71±0.03	1.50±0.10	-4.49±0.05	-0.96±0.07	-2.05±0.22
IGUA	1.54±0.05	0.99±0.08	-0.47±0.23	-4.35±0.07	-1.18±0.11	1.98±0.34
YAIG	0.83±0.02	0.77±0.03	0.77±0.08	-1.97±0.05	-1.47±0.10	2.90±0.26
ZIHP	2.02±0.04	1.89±0.06	-0.22±0.18	-2.04±0.06	-1.33±0.09	-6.00±0.26
PINO	2.13±0.06	1.92±0.08	1.14±0.24	-2.50±0.09	-0.60±0.13	-7.20±0.38
OAXA	2.24±0.09	1.63±0.13	-1.58±0.38	-2.20±0.12	-2.34±0.18	3.28±0.50

Figure Captions

Fig. 1. (Top) Location of permanent GPS sites in and near the Guerrero seismic gap, Mexico. The vectors at the sites indicate horizontal position change for a year of interseismic, steady-state strain accumulation phase (dark arrows) and during the January-April, 2002 slow-slip (white arrows). The vectors near the mid-America trench (MAT) illustrate velocity of COCOS plate relative to NOAM plate. Large rectangle is the horizontal projection of the plate interface over which the slip was inverted from the GPS data. The rectangle is divided in (3x4) elements. The element number is shown in parentheses. Guerrero gap coincides with elements *(2,j)*. (Bottom) Idealized geometry of the Benioff zone along AA' used in the inversion. The white and the dark segments of the interface indicate the element widths.

Fig. 2. Time series of the position of *CAYA* station for the interval from January 1997 to July 2003. Shaded rectangles show the two silent events recorded by the station. (Modified from Kostoglodov et al. [**6**])

Fig. 3. (Top) Slip distribution on the plate interface obtained from inversion of the GPS data during the slow-slip phase (January-April, 2002; 4 months). The area in the figure corresponds to the rectangle shown in Figure 1. The numbers in parentheses indicate elements as in Figure 1 (top). Elements separated by dashed lines have been merged. Vectors shown by continuous and dashed lines indicate observed and calculated displacements, respectively. For clarity, vertical components are shown to the right side of the figure. (Middle) Same as top but with elements (2,2) and (2,3) merged together. (Bottom) Same as middle but for the steady-state velocities.

Fig. 4. Cumulative seismic moment release curve for the Guerrero region; modified from Anderson et al. **[22]**. Slopes of the parallel lines, both of which envelop the curve, correspond to 100% seismic coupling (α=1.0, continuous lines) and 70% coupling (α=0.7, dashed lines) (see text).

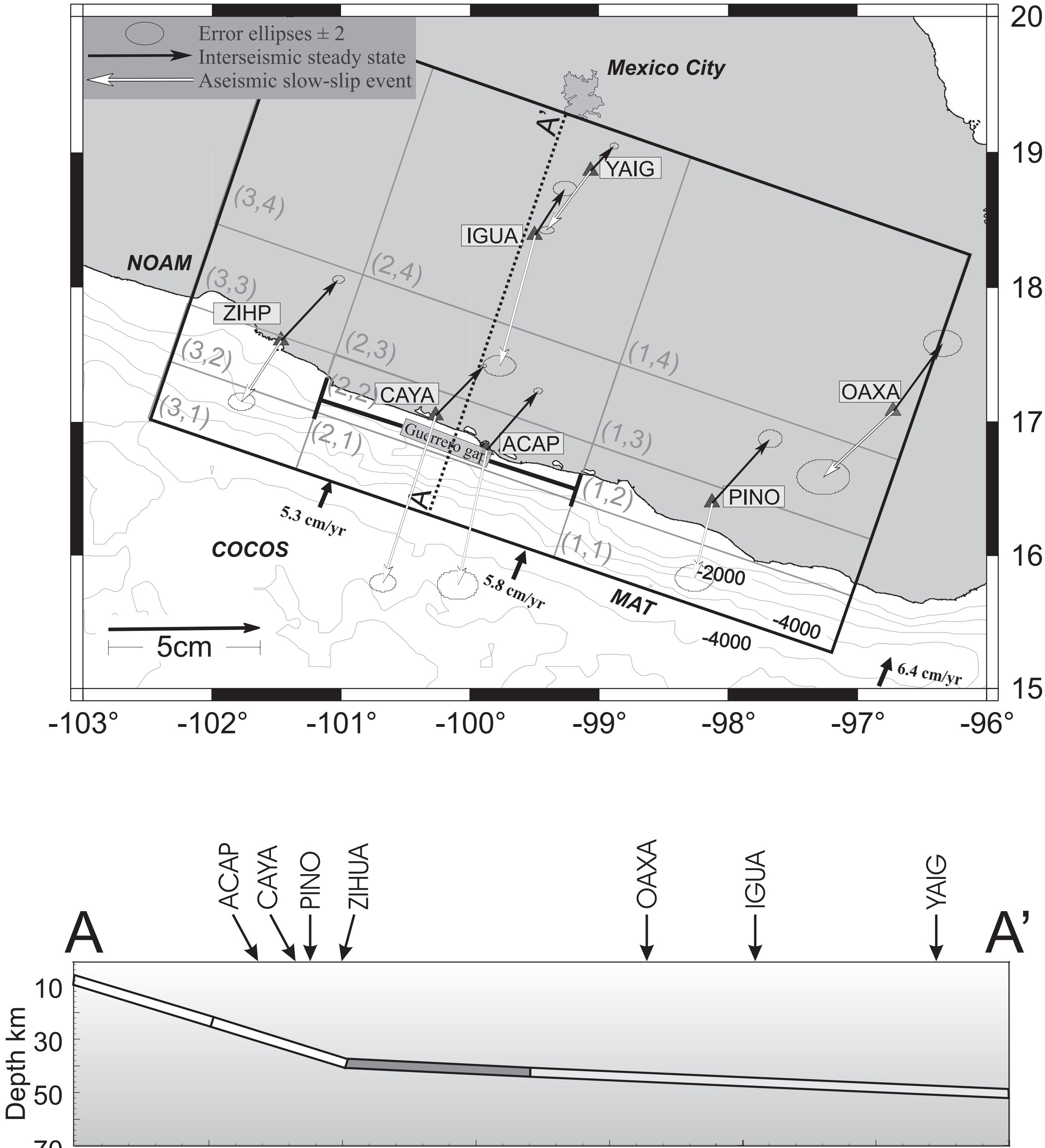

Error ellipses ± 2
Interseismic steady state
Aseismic slow-slip event
Mexico City
A'
YAIG
IGUA
NOAM
ZIHP
CAYA
ACAP
Guerrero gap
OAXA
PINO
COCOS
MAT
5.3 cm/yr
5.8 cm/yr
6.4 cm/yr
-2000
-4000
-4000
5cm
A
20°
19°
18°
17°
16°
15°
-103°
-102°
-101°
-100°
-99°
-98°
-97°
-96°
ACAP
CAYA
PINO
ZIHUA
OAXA
IGUA
YAIG
A
A'
Depth km
Distance from the trench km

Figure 1

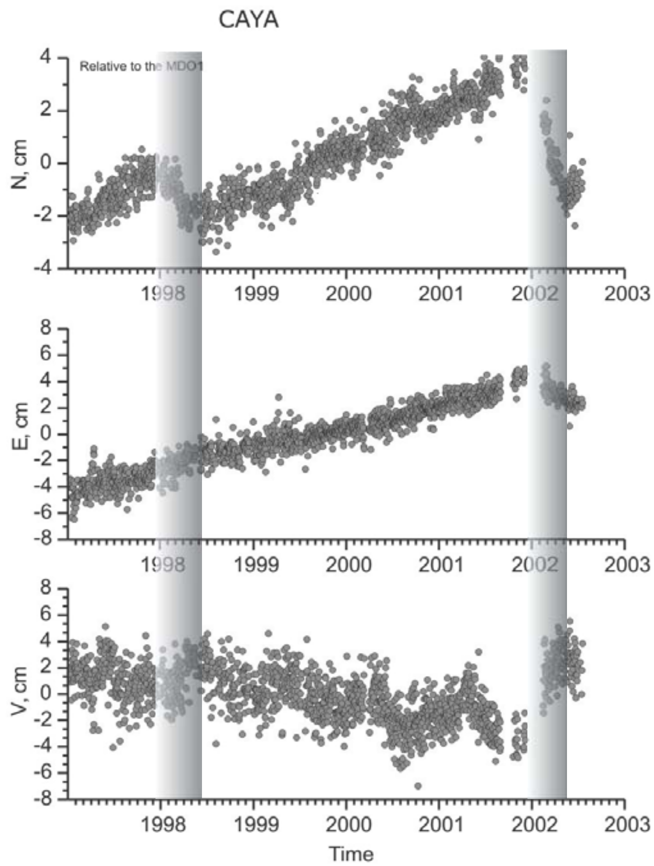
CAYA
Relative to the MDO1
N, cm
E, cm
V, cm
1998
1999
2000
2001
2002
2003
Time

Figure 2

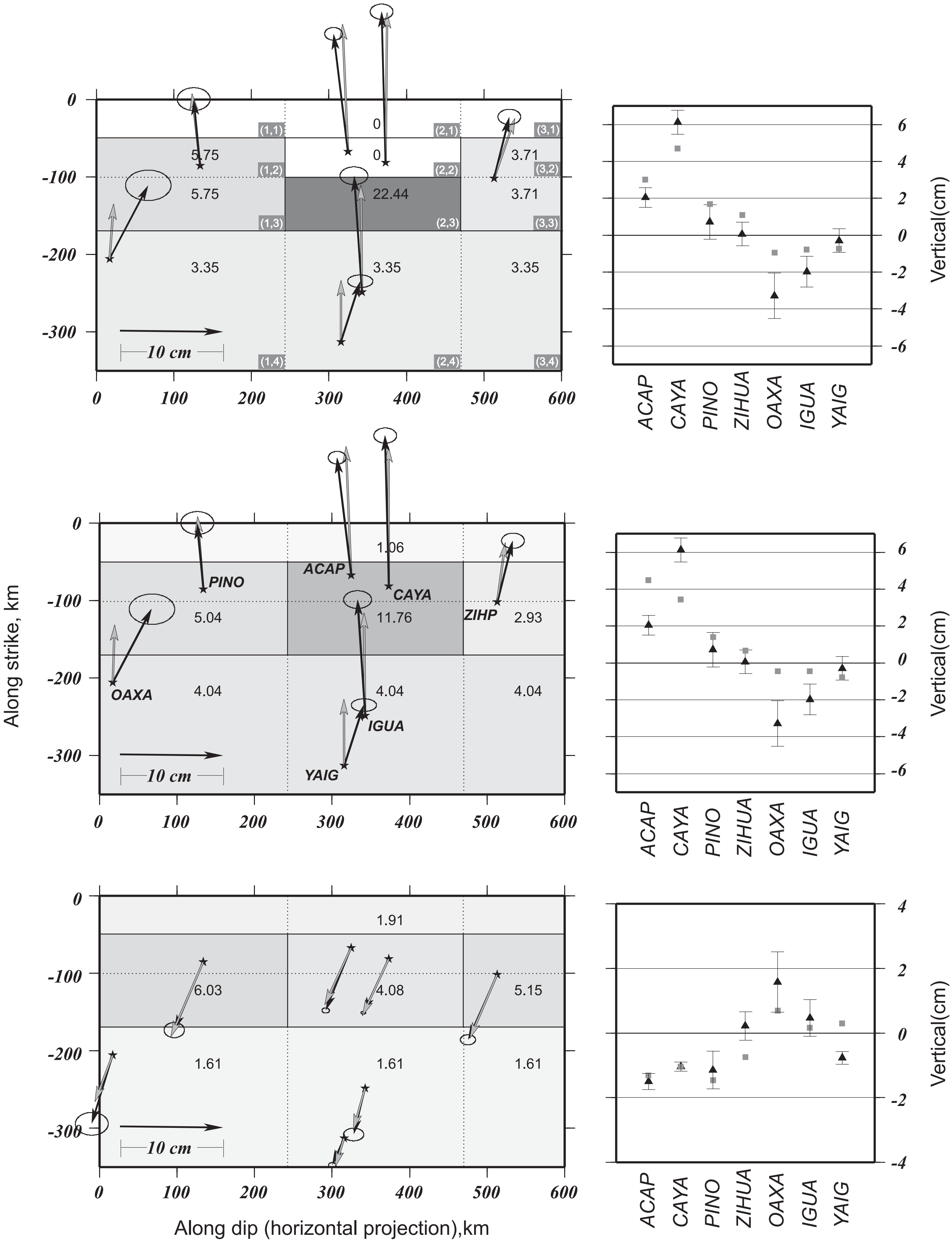

(1,1)
(2,1)
(3,1)
(1,2)
(2,2)
(3,2)
(1,3)
(2,3)
(3,3)
(1,4)
(2,4)
(3,4)
0
5.75
0
3.71
5.75
22.44
3.71
3.35
3.35
3.35
10 cm
Vertical(cm)
ACAP
CAYA
PINO
ZIHUA
OAXA
IGUA
YAIG
Along strike, km
PINO
ACAP
CAYA
ZIHP
OAXA
IGUA
YAIG
1.06
5.04
11.76
2.93
4.04
4.04
4.04
1.91
6.03
4.08
5.15
1.61
1.61
1.61
Along dip (horizontal projection),km

Figure 3

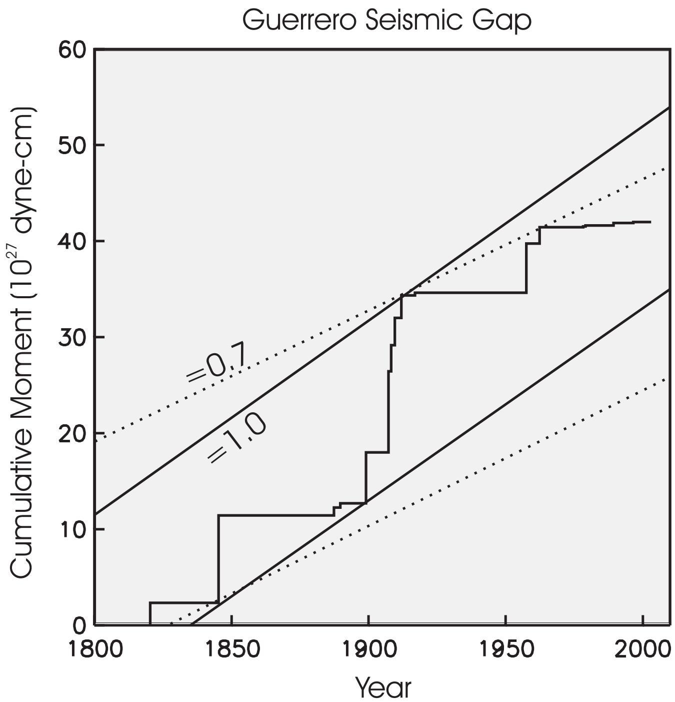
Guerrero Seismic Gap
Cumulative Moment (10^{27} dyne-cm)
Year
0
10
20
30
40
50
60
1800
1850
1900
1950
2000
=0.7
=1.0

Figure 4